Interface Focus

rsfs.royalsocietypublishing.org

Research

Cite this article: Xia X, Li W, Zhang Y, Xia Y. 2013 Silica-coated dimers of silver nanospheres as surface-enhanced Raman scattering tags for imaging cancer cells. Interface Focus 3: 20120092.
http://dx.doi.org/10.1098/rsfs.2012.0092

One contribution of 10 to a Theme Issue 'Molecular-, nano- and micro-devices for real-time *in vivo* sensing'.

Subject Areas:
biotechnology

Keywords:
surface-enhanced Raman scattering, surface-enhanced Raman scattering tag, dimer, hot spot, cancer cell, imaging

Author for correspondence:
Younan Xia
e-mail: younan.xia@bme.gatech.edu

Electronic supplementary material is available at http://dx.doi.org/10.1098/rsfs.2012.0092 or via http://rsfs.royalsocietypublishing.org.

Royal Society Publishing
Informing the science of the future

Silica-coated dimers of silver nanospheres as surface-enhanced Raman scattering tags for imaging cancer cells

Xiaohu Xia[1], Weiyang Li[2], Yu Zhang[1] and Younan Xia[1]

[1]The Wallace H. Coulter Department of Biomedical Engineering, Georgia Institute of Technology and Emory University Medical School; School of Chemistry and Biochemistry, School of Chemical and Biomolecular Engineering, Georgia Institute of Technology, Atlanta, GA 30332, USA
[2]Department of Materials Science and Engineering, Stanford University, Stanford, CA 94305, USA

Surface-enhanced Raman scattering (SERS) tags have been actively explored as a multiplexing platform for sensitive detection of biomolecules. Here, we report a new type of SERS tags that was fabricated by sequentially functionalizing dimers made of 50 nm Ag nanospheres with 4-mercaptobenzoic acid as the Raman reporter molecule, silica coating as a protective shell and antibody as a targeting ligand. These dimer-based tags give highly enhanced and reproducible Raman signals owing to the presence of a well-defined SERS hot spot at the junction between two Ag nanospheres in the dimer. The SERS enhancement factor (EF) of an individual dimer tag supported on a glass slide can reach a level as high as 4.3×10^6. In comparison, the EFs dropped to 2.8×10^5 and 8.7×10^5, respectively, when Ag nanospheres and nanocubes with sizes similar to the spheres in the dimer were used to fabricate the tags using similar procedures. The SERS signals from aqueous suspensions of the dimer-based tags also showed high intensity and good stability. Potential use of the dimer-based tags was demonstrated by imaging cancer cells overexpressing HER2 receptors with good specificity and high sensitivity.

1. Introduction

Surface-enhanced Raman scattering (SERS) [1–4] has a number of advantages for analytical applications: high sensitivity, narrow spectral bandwidth, absence of photobleaching and single laser excitation for detection of multiple labels [5–9]. A common use of SERS for quantitative analysis is based on SERS tags [10–14], which can be fabricated by placing Raman reporter molecules on the surface of a metal nanoparticle (typically made of Ag or Au) to provide a simple way to code the surface property (e.g. the type of receptor or ligand) of tag with a known SERS spectrum. A protective shell (made of SiO_2, or polymers) is then coated on the particle surface to prevent undesired interactions between the metal core and the environment. Finally, targeting ligands (e.g. antibodies and biotin) are conjugated to the protective shell. Quantitative analysis of a specific analyte, using a SERS tag, relies on the specific binding between the analyte and the targeting ligand and the detection of SERS signals from the Raman reporter molecules.

Among various components of a SERS tag, the metal core is responsible for Raman signal enhancement and thus mainly determines the detection sensitivity and reproducibility of a tag. A number of SERS tags have been reported in the literature, demonstrating the benefits of different metal cores. Spherical Ag and Au nanoparticles are the most commonly used cores owing to their facile synthesis and commercial availability [7,12,15–17]. However, these spherical nanoparticles produce relatively weak Raman signals (with an enhancement factor (EF) on the order of 10^4–10^6) [18,19] and thus offer relatively low detection sensitivity when used for SERS tags. In general, this limitation in enhancement can be overcome by coupling the spherical nanoparticles to form aggregates, such as dimers and trimers. In comparison with single nanoparticles, coupled nanoparticles can further increase the Raman signal by several orders of magnitude (up to 10^{10}–10^{14}) owing to the hot spots, which are extremely small regions with drastically

intensified E-fields located at the junctions between nanoparticles [20–23]. In this regard, different types of coupled nanoparticles have been prepared for the use of fabricating highly sensitive SERS tags [24–29]. In most cases, preparation of coupled nanoparticles relies on the random aggregation of metal nanoparticles as induced by Raman reporter molecules or other linker molecules. The random aggregation, however, always leads to poor controllability and reproducibility for the resultant SERS tags. Furthermore, the linker molecules bridging the two adjacent nanoparticles tend to prevent the Raman reporter molecules from entering the hot spot regions. Therefore, preparation of coupled nanoparticles with well-defined hot spots that can ensure both sensitivity and reproducibility for a SERS tag remains a challenge.

Recently, our group has successfully synthesized dimers of Ag nanospheres with a uniform distribution in terms of both size and shape by controlling the colloidal stability with the addition of ionic species [30]. Experimental data have shown that Raman reporter molecules, such as 4-methylbenzenethiol, could be readily trapped in the hot spot region, ensuring a highly enhanced Raman signal [30,31]. In this study, we further demonstrated the use of this well-defined dimer of Ag nanospheres for the preparation of a new SERS tag by sequentially functionalizing the surface of the dimers with 4-mercaptobenzoic acid (4-MBA) as the Raman reporter molecule, silica coating as a protective shell and antibodies as targeting ligands. To better understand how the geometric shape of a metal role influences the performance of a SERS tag, we also performed a comparison study by using Ag nanospheres and nanocubes with roughly similar sizes to the metal cores for SERS tags. In the following discussion, the three different types of SERS tags fabricated from dimers of Ag nanospheres, Ag nanospheres and Ag nanocubes will be referred to as dimer tags, sphere tags and cube tags, respectively, for the purpose of simplicity. We found that the dimer tags gave the strongest Raman signal compared with the other two types of tags in both substrate-supported and solution-phase measurements. Potential use of the dimer tags was demonstrated by imaging cancer cells, which overexpress HER2 receptors on the surfaces, with high sensitivity and good specificity.

2. Methods

2.1. Chemicals and materials

4-MBA (99%), 1,4-benzenedithiol (1,4-BDT, 99%), poly(vinyl pyrrolidone) (PVP, MW $\approx$ 55 000), ferric nitrate nonahydrate ($Fe(NO_3)_3{\cdot}9H_2O$, 99.99%), tetraethylorthosilicate (TEOS $\geq$ 99.0%), (3-aminopropyl) trimethoxylsilane (APTMS, 97%), dextran 500 (MW $\approx$ 500 000) were ordered from Sigma-Aldrich (St. Louis, MO, USA). Mouse anti-HER2 antibody (clone no. CB11) was purchased from Invitrogen (Carlsbad, CA, USA). SK-BR-3 human adenocarcinoma cells and U-87 MG human glioblastoma cells were obtained from ATCC (Manassas, VA, USA). All aqueous solutions were prepared using deionized (DI) water with a resistivity of 18.2 MΩ·cm. All the reactions for etching of Ag nanocubes and silica coating were carried out in glass vials (20 ml, VWR International).

2.2. Synthesis of silver nanoparticles

Silver nanocubes of 50 and 60 nm in edge length were synthesized, using the recently reported polyol method, with ethylene glycol serving as the solvent and CF_3COOAg as a precursor to elemental silver [32]. Dimers of Ag nanospheres were prepared by etching 60 nm Ag nanocubes with $Fe(NO_3)_3$ solution in ethanol as reported in our recent publication with some modifications [30]. Briefly, 20 µl of 60 nm Ag nanocubes (5 nM in particle concentration) was added into 3 ml of ethanol containing 20 mg of PVP. The suspension was then mixed with 50 µl of 10 mM $Fe(NO_3)_3$ aqueous solution under stirring. After 1 h, the final product was washed three times with ethanol. The Ag nanospheres of 50 nm in diameter were prepared by etching 60 nm Ag nanocubes with a low concentration of $Fe(NO_3)_3$ in an aqueous solution, according to our previously reported procedure [33].

2.3. Preparation of surface-enhanced Raman scattering tags

Preparation of the dimer tags is schematically illustrated in figure 1. The procedure can be divided into the following major steps: (i) *Functionalization with 4-MBA:* 4-MBA ethanol solution (50 µl, 1 mM) was added into 3 ml of ethanol containing 3 mg of PVP and approximately 3.5×10^{10} dimers of Ag nanospheres. After incubation for 1 h, the product was washed with ethanol once and re-dispersed in 3 ml of ethanol. (ii) *Silica coating:* 250 µl of H_2O, 70 µl of 29 per cent ammonia solution and 4 µl of TEOS were sequentially added into the 4-MBA-functionalized dimers. After stirring for 3 h, the resultant silica-coated dimers were washed twice with DI water. (iii–v) *Antibody conjugation:* prior to conjugation, amino groups were introduced to the surface of silica-coated Ag dimers by treatment with APTMS. Anti-HER2 antibodies were then covalently linked to the aminated dimers through oxidized dextran 500 [34]. Detailed protocol for antibody conjugation is provided in the electronic supplementary material. The sphere and cube tags were prepared by using a procedure similar to the one used for the dimer tags, except for the use of 50 nm Ag nanospheres and nanocubes as the metal cores, respectively.

2.4. Cell culture and targeting

SK-BR-3 cells were maintained in McCoy's 5A medium (ATCC), supplemented with 10 per cent foetal bovine serum (FBS, ATCC) and 1 per cent penicillin–streptomycin (P/S, Invitrogen). U-87 cells were maintained in Eagle's minimum essential medium (ATCC), supplemented with 10 per cent FBS and 1 per cent P/S. All cultures were kept in an incubator at 37°C in a humidified atmosphere containing 5 per cent CO_2, and the medium was changed every other day. The SK-BR-3 and U-87 cells were seeded onto sterile cover glasses in the wells of a 24-well plate, at a density of 5×10^3 cells/well and left to attach overnight. The cells were then fixed with 4 per cent formaldehyde for 10 min. After washing with phosphate-buffered saline (PBS, Invitrogen) twice, the cells were blocked with 2 ml of PBS solution containing 1.5 per cent bovine serum albumin (BSA, Sigma) for 1 h. The cells were then incubated with SERS tags (50-fold dilution, i.e. 1.4×10^{10} tags/well) in the above-mentioned blocking solution for 2 h. After rinsing with PBS buffer twice, the cover glasses were finally sealed with a glass coverslip prior to the SERS measurements.

2.5. Surface-enhanced Raman scattering measurements

SERS spectra were recorded using a Renishaw in via confocal Raman spectrophotometer coupled to a Leica microscope with a 50 × objective (NA = 0.90) in backscattering configuration. The light sources at 514 and 785 nm were generated from an argon continuous wave (CW) laser and a semiconductor CW diode laser, respectively, and used with a holographic notch filter based on a grating of 1200 lines per millimetre. SERS spectra from individual SERS tags supported on a glass slide were acquired with λ_{ex} = 514 nm, t = 20 s and P_{laser} = 0.4 mW; SERS spectra from aqueous suspensions of SERS tags were acquired with λ_{ex} = 514 nm, t = 20 s and P_{laser} = 2 mW. Sample cells for the suspensions were

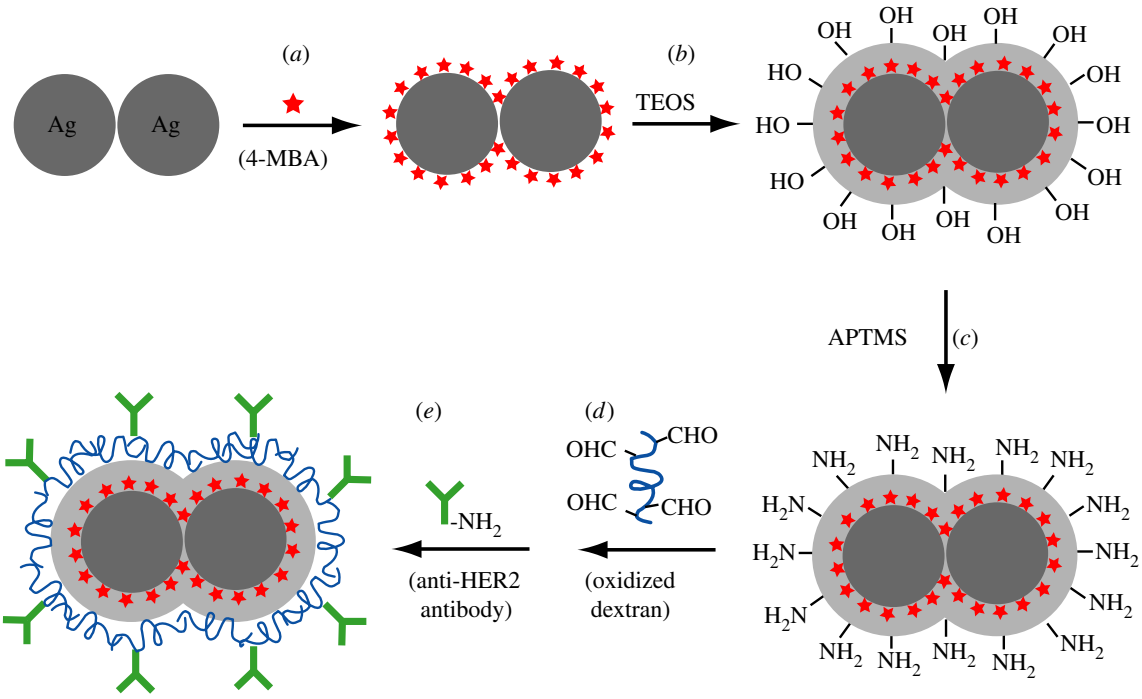

Figure 1. Schematic of the major steps involved in the preparation of the dimer-based SERS tag: (*a*) a dimer of Ag nanospheres was functionalized with a self-assembled monolayer of 4-MBA to be used as the Raman reporter molecule; (*b*) the 4-MBA-functionalized dimer of Ag nanospheres was then coated with a silica shell; (*c*) the surface of the silica shell was derivatized with amino groups using APTMS; and (*d*,*e*) antibodies were covalently conjugated to the surface of aminated silica shell through the Schiff reaction with oxidized dextran 500 as a linker.

constructed by attaching the cap of a microcentrifuge tube to a glass slide. The cap served as a vessel for the liquid sample, and a glass coverslip (approx. 0.15 mm) was carefully placed on top to prevent solvent evaporation and to serve as a reference point from which the focal point was lowered to a depth of 0.2 mm into the sample; SERS imaging of cancer cells was acquired using a point-mapping method. This procedure generated a spectral image by measuring the Raman spectrum of each pixel of the image, one at a time, to obtain a SERS image showing the distribution of the SERS tags attached to the cancer cell. SERS signals were collected by point mapping 24 × 24 µm areas, with 2.0 µm steps, and $\lambda_{ex} = 514$ nm, $t = 10$ s and $P_{laser} = 2$ mW for each point measurement. The intensities of SERS peak at 1588 cm^{-1} were chosen for generating SERS mapping image with user-defined Matlab (MathWorks) programs. OriginLab software (Northampton, MA, USA) was used for SERS spectra baseline correction.

2.6. Instrumentation

Transmission electron microscopy (TEM) images of nanoparticles were taken using a Tecnai G2 spirit twin microscope (FEI, Hillsboro, OR, USA) operated at 120 kV. Scanning electron microscopy (SEM, Nova NanoSEM 230, FEI) was used to characterize SERS tags supported on substrates after SERS measurements. Prior to SEM imaging, the samples were sputter-coated with gold for 60 s. The concentration of Ag was determined using inductively coupled plasma mass spectrometry (ICP-MS; Perkin-Elmer Elan DRC II ICP-MS), and then converted to the concentration of Ag nanoparticles once the particle size and morphology had been determined by TEM imaging. Extinction spectra of all the nanoparticles were recorded, using a UV–vis spectrometer (Varian, Cary 50).

3. Results and discussion

3.1. Preparation and characterization of the dimer tags

The dimer tags were prepared by sequentially coating dimers of Ag nanospheres that were 50 nm in size (defined by the average diameter of the two constituent spheres; electronic supplementary material, figure S1*a*) with 4-MBA, silica shell and antibodies, as shown in figure 1. We chose 4-MBA as the Raman reporter molecule (figure 1*a*) because (i) it is known to form a stable, well-defined monolayer on Ag surfaces with a known molecule footprint through the Ag–S linkage [35,36]; (ii) it has a relatively large Raman scattering cross section and SERS peaks that have been well characterized [37]; and (iii) these molecules are expected to be able to penetrate the hot spot regions between the two Ag spheres owing to their relatively small size [30,31]. After the 4-MBA-functionalized dimers of Ag nanospheres had been coated with silica shells (figure 1*b*), amino groups were introduced into the surface by treating with APTMS under gentle conditions (figure 1*c*) [34,38]. The existence of amino groups on the silica shell was confirmed by using the salicylaldehyde-mediated yellow colour change [38]. Finally, antibodies were covalently conjugated to the aminated surface by using oxidized dextran 500 as a linker (figure 1*d*), with which the silica shell and antibodies were coupled through the Schiff reaction (figure 1*e*). We decided to use oxidized dextran 500 for two reasons: (i) it offers a large number of active groups for antibody conjugation and (ii) it can help increase hydrophilicity of the resultant dimer tags, rendering it more easily dispersible in aqueous solution [34,38].

Figure 2*a* shows a TEM image of the as-prepared dimer tags with a uniform size and shape. A magnified TEM image of an individual dimer tag (inset of figure 2*a*) clearly shows that the metallic core of the tag consists of two Ag spheres with a smooth surface. No obvious change in both shape and size was observed for the dimers of Ag nanospheres before (see the electronic supplementary material, figure S1*a*) and after surface coatings (figure 2*a*). The strong contrast difference between Ag and SiO_2 suggests that the silica shell had a thickness of approximately 15 nm over the

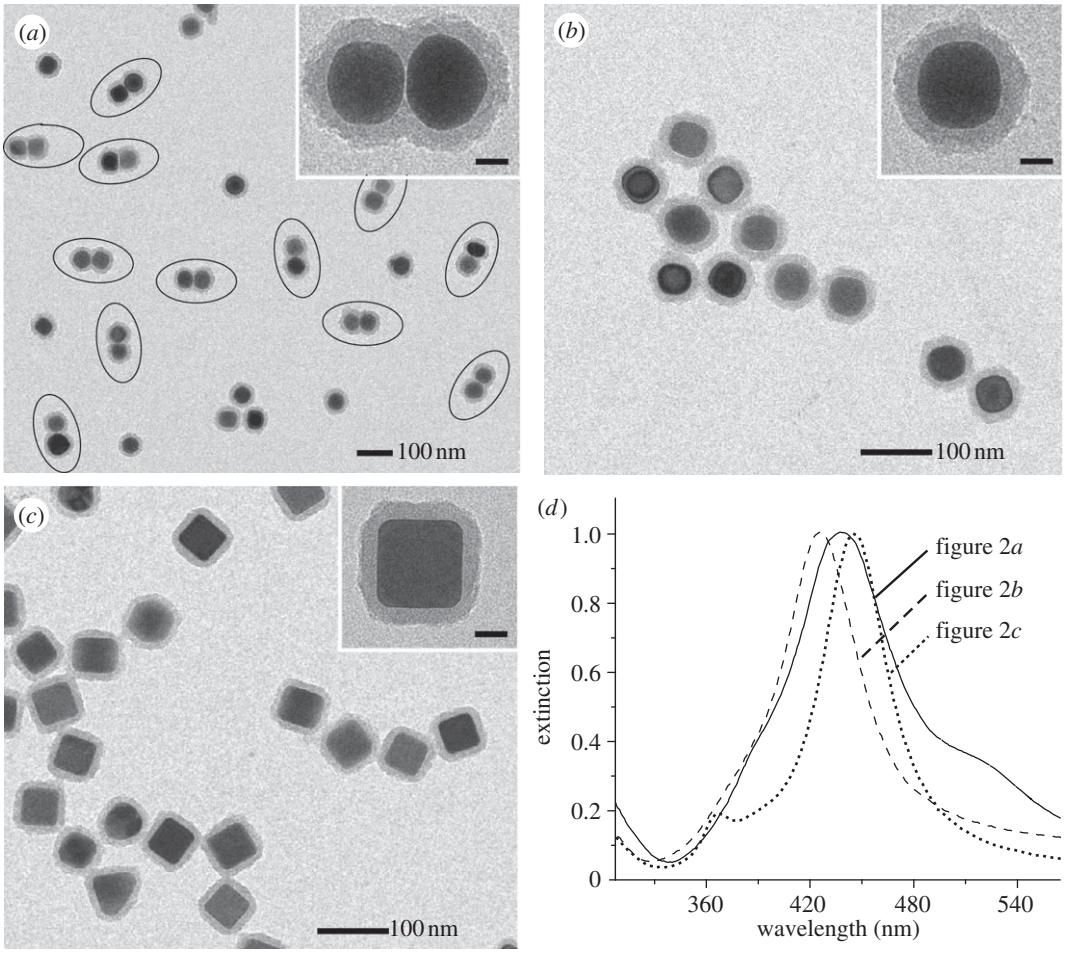

Figure 2. TEM images of (*a*) dimer tags, (*b*) sphere tags and (*c*) cube tags. The insets show TEM images of individual tags at a higher magnification. Scale bars in the insets of (*a–c*) are 20 nm. (*d*) UV–vis extinction spectra of the tags shown in (*a–c*).

entire surface of the dimeric core. By counting over 200 particles on TEM images with lower magnifications (see the electronic supplementary material, figure S2), we found that the yield of the dimer tag (the number of tags with dimeric cores divided by the total number of tags with either dimeric or spherical cores) was approximately 65 per cent. For comparison studies, we also used 50 nm Ag nanospheres (see the electronic supplementary material, figure S1*c*) and nanocubes (see the electronic supplementary material, figure S1*d*) as metal cores for the preparation of sphere and cube tags, respectively, by using the same procedures for surface silica coating and conjugation. Figure 2*b*,*c* shows TEM images of the sphere and cube tags, respectively. The magnified TEM images of individual sphere and cube tags in the insets of figure 2*b* and *c*, respectively, indicated that the core of the sphere tag had a smooth and round profile, whereas the core of the cube tag contained relatively sharp edges and corners. Silica shells with thicknesses of approximately 15 nm were also observed for both the sphere and the cube tags.

It is worth pointing out that the thickness of the silica shell could be easily controlled by simply varying the amount of TEOS added during the coating process. For example, the use of 1, 2, 5 and 10 µl of TEOS in a standard procedure for coating Ag nanospheres resulted in the formation of silica shells 5, 10, 20 and 45 nm, respectively, in thickness (electronic supplementary material, figure S3). Also, we found that addition of PVP is critical to the formation of a uniform silica shell. Using the coating of Ag nanocubes as an example, we found that irregular silica layers were formed over the nanocubes (electronic supplementary material, figure S4*a*) in the absence of PVP. In the presence of PVP, however, a relatively smooth and homogeneous silica shell was observed on the surface of the same type of nanocubes (see the electronic supplementary material, figure S4*b*). These observations indicate that PVP can serve as both stabilizing and coupling agents in coating Ag nanoparticles with silica shells [39,40].

Figure 2*d* shows UV–vis spectra of the three different types of SERS tags. The localized surface plasmon resonance (LSPR) peaks of the three tags were all slightly red-shifted compared with the spectra of pristine Ag particles (see the electronic supplementary material, figure S1*d*). The positions of the major LSPR peaks of the SERS tags were located in roughly the same region (420–450 nm). In contrast to the sphere tags, a small shoulder peak near 520 nm (next to the major peak) can be resolved for the dimer tags, indicative of dimerization. This observation is consistent with our previous LSPR study on Ag dimers consisting of 30 nm Ag spheres [31].

3.2. Surface-enhanced Raman scattering properties of the dimer tag

We first measured the SERS spectra of individual dimer tags supported on a glass slide with 514 nm laser excitation. After SERS measurements, we used SEM to obtain information about the size, shape and orientation of each tag, in a process known as SERS–SEM correlation [41]. Figure 3*a* shows the SERS spectra taken from a single dimer tag, with the angles between laser polarization and longitudinal axis of the

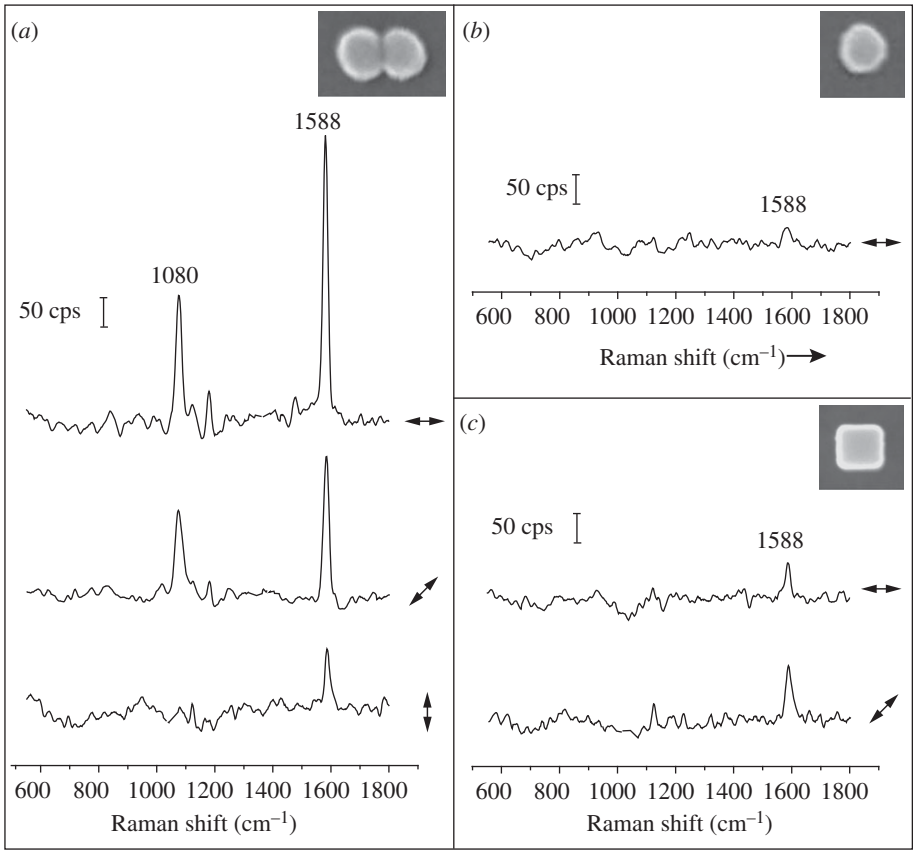

Figure 3. SERS spectra recorded from individual SERS tags supported on glass slides: (*a*) dimer tags, (*b*) sphere tags and (*c*) cube tags. The double arrows beside each spectrum denote the direction of laser polarization relative to the particle orientation shown in the insets of (*a*–*c*), which are the SEM images of the corresponding tags from which the spectra were recorded.

dimer being at 0° (top trace), 45° (middle trace) and 90° (bottom trace). The two strong peaks of the spectra located at 1080 and 1588 cm^{-1}, assigned to the 8a and 12 vibrational mode of phenyl ring-stretching motion, respectively, are the characteristic peaks for 4-MBA [37]. The 4-MBA signals were strongly dependent on laser polarization. It can be observed that the 4-MBA peaks were maximized when the laser was polarized parallel to the longitudinal axis of the dimer tag. The 4-MBA signal was gradually reduced when the laser was rotated by 45° and 90° away from the longitudinal axis of dimer tag. At 90°, the intensity of the peak at 1588^{-1} cm was reduced by a factor of approximately 15.

In comparison, the 4-MBA signal from an individual sphere (figure 3*b*) or cube tag (figure 3*c*) was much weaker than that from the dimer tag (figure 3*a*). For the cube tag, we found that the 4-MBA signal from a cube orientated with a side diagonal axis parallel to the laser polarization was about two times higher than the configuration when the cube was oriented with one of the edges parallel to the laser polarization. This observation is consistent with the results for Ag nanocubes obtained in our previous work [42]. It can be concluded that the intensities of 4-MBA signals from individual tags supported on glass slides decreased in the order of dimer tag (parallel) $\gg$ cube tag (diagonal) $>$ sphere tag. We also recorded the SERS signals from the tags in aqueous suspensions with the same particle concentrations. In this case, the acquired SERS signals represent an average from all different particle orientations. As shown in figure 4, the intensities of the 4-MBA signals from the aqueous suspensions of tags were found to follow a similar trend in the order of dimer tag $\gg$ cube tag $>$ sphere tag.

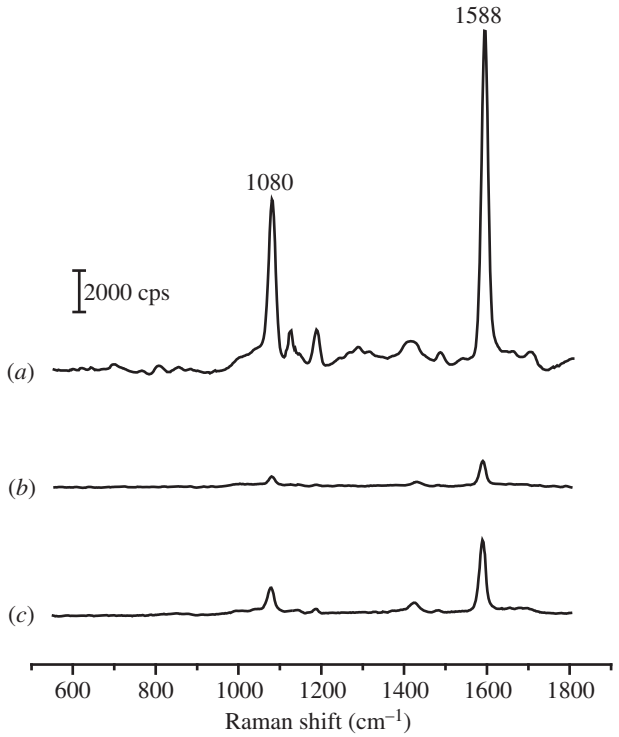

Figure 4. SERS spectra recorded from aqueous suspensions of: (*a*) dimer tags, (*b*) sphere tags and (*c*) cube tags. The particle concentrations of the tags were approximately 100 pM for all samples.

To quantitatively compare the SERS enhancements between these tags, we used the peak at 1588 cm^{-1} (the strongest band in the 4-MBA spectra) to calculate the SERS EF for

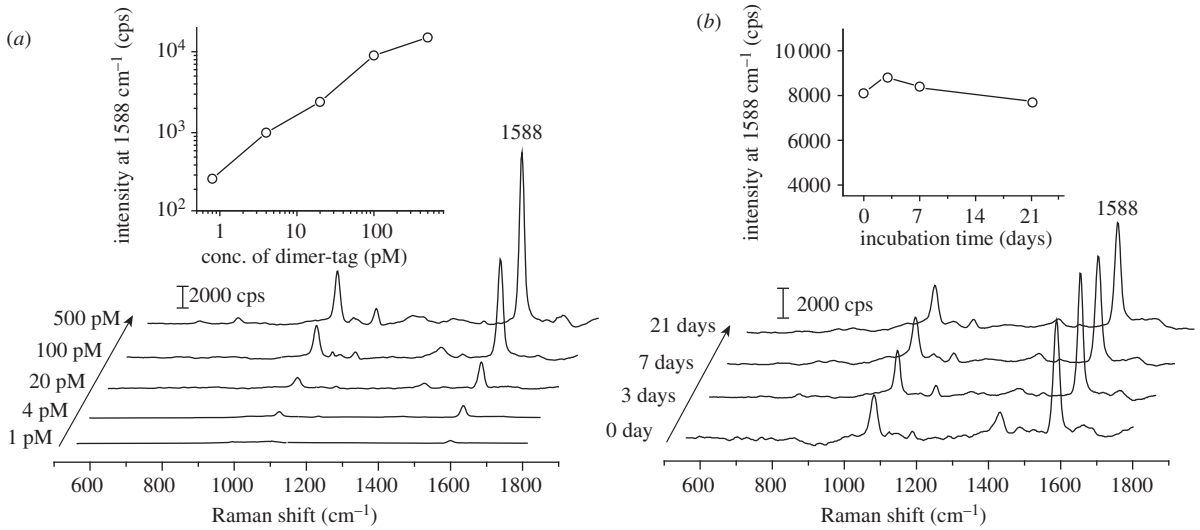

Figure 5. (*a*) SERS spectra recorded from aqueous suspensions of the dimer tags with different particle concentrations ranging from 1 to 500 pM. The inset is a plot of SERS intensity of 4-MBA band at 1588 cm^{-1} as a function of particle concentration. (*b*) SERS spectra recorded from a 100 pM aqueous suspension of the dimer tag after they had been incubated in DI water for different periods of time. The inset is a plot of the SERS intensity of 4-MBA band at 1588 cm^{-1} as a function of incubation time.

Table 1. The EFs of individual SERS tags supported on glass slides ($EF_{substrate}$) and EFs of different tags in aqueous suspensions ($EF_{solution}$). Each value of EF represents an average of the data from six independent experiments. The double arrow above the drawings of tags denotes the direction of laser polarization.

↔	$EF_{substrate}$	$EF_{solution}$
	4.3×10^6	
	1.7×10^6	9.8×10^5
	6.6×10^5	
	2.8×10^5	1.4×10^5
	4.5×10^5	
	8.7×10^5	2.4×10^5

each tag using the following equation [43,44]

$$\mathrm{EF} = \frac{I_{\mathrm{SERS}} \times N_{\mathrm{bulk}}}{I_{\mathrm{bulk}} \times N_{\mathrm{SERS}}},$$

where I_{SERS} and I_{bulk} are the intensities of the same band for the SERS and bulk spectra, N_{bulk} is the number of molecules probed for a bulk sample and N_{SERS} is the number of molecules probed with SERS. N_{bulk} was determined based on the ordinary Raman spectrum of a 0.1 M 4-MBA solution in 12 M aqueous NaOH and the focal volume of our Raman system (1.48 pl). When determining N_{SERS}, we assumed that the 4-MBA molecules were adsorbed as a monolayer with a molecular footprint of 0.33 nm^2 [36], and a surface area of 15 700, 7 850, 15 000 nm^2 was calculated for dimer, sphere and cube tags, respectively, based on their shape and size (figure 1*a–c*). Table 1 summarizes the EFs for these tags with various laser polarizations. The EFs of dimer tags for both substrate-supported and solution-dispersed configurations were much higher than that of sphere tags. In addition, the EFs of cube tags were slightly larger than that of sphere tags. If we take into account the differences in interparticle gaps, corners and edges in the metal core of a tag where SERS hot spots tend to be formed [45], the observed differences in EF are easy to understand. The dimer tag with a dimer core contains an interparticle gap and is thus expected to offer intense hot spot enhancement. Therefore, it should give the strongest SERS signals. Hot spots could also be created at the corner sites of a cubic core of the cube tags [42,46], leading to a higher EF than the sphere tags with spherical cores. Because the three types of tags had a similar major LSPR peak (figure 2*d*), the possibility of wavelength-dependent enhancement [43], where the SERS activity is maximized when the excitation source matched the LSPR peak of the tags, could be neglected.

We also investigated the sensitivity and stability of aqueous suspensions of the dimer tags. As shown in figure 5*a*, dimer tags at a certain particle concentration (in the range of 1–500 pM) produced consistent SERS peaks of 4-MBA under identical measuring conditions. As shown in the inset of figure 5*a*, there is a linear dependence between the intensity of the band of 4-MBA at 1588 cm^{-1} and the concentration of dimer tag. To test the stability of the dimer tag, we recorded SERS spectra from an aqueous suspension of the dimer tag as a function of time. As shown in figure 5*b*, the SERS spectra recorded at different time points with a period of three weeks only showed some minor variations in terms of both intensity (the inset of figure 5*b*) and peak position. It should be pointed out that (i) other small molecules such as 1,4-benzenedithiol (1,4-BDT) [44], in addition to 4-MBA, can also serve as the Raman reporter molecule for the dimer tag (see the electronic supplementary material, figure S5), indicating the capability to label the dimers with multiple tag molecules; and (ii) an intense signal could be detected from aqueous suspension of the dimer tag under 785 nm laser excitation with a SERS EF of approximately 1.7×10^5 (see the electronic supplementary material, figure

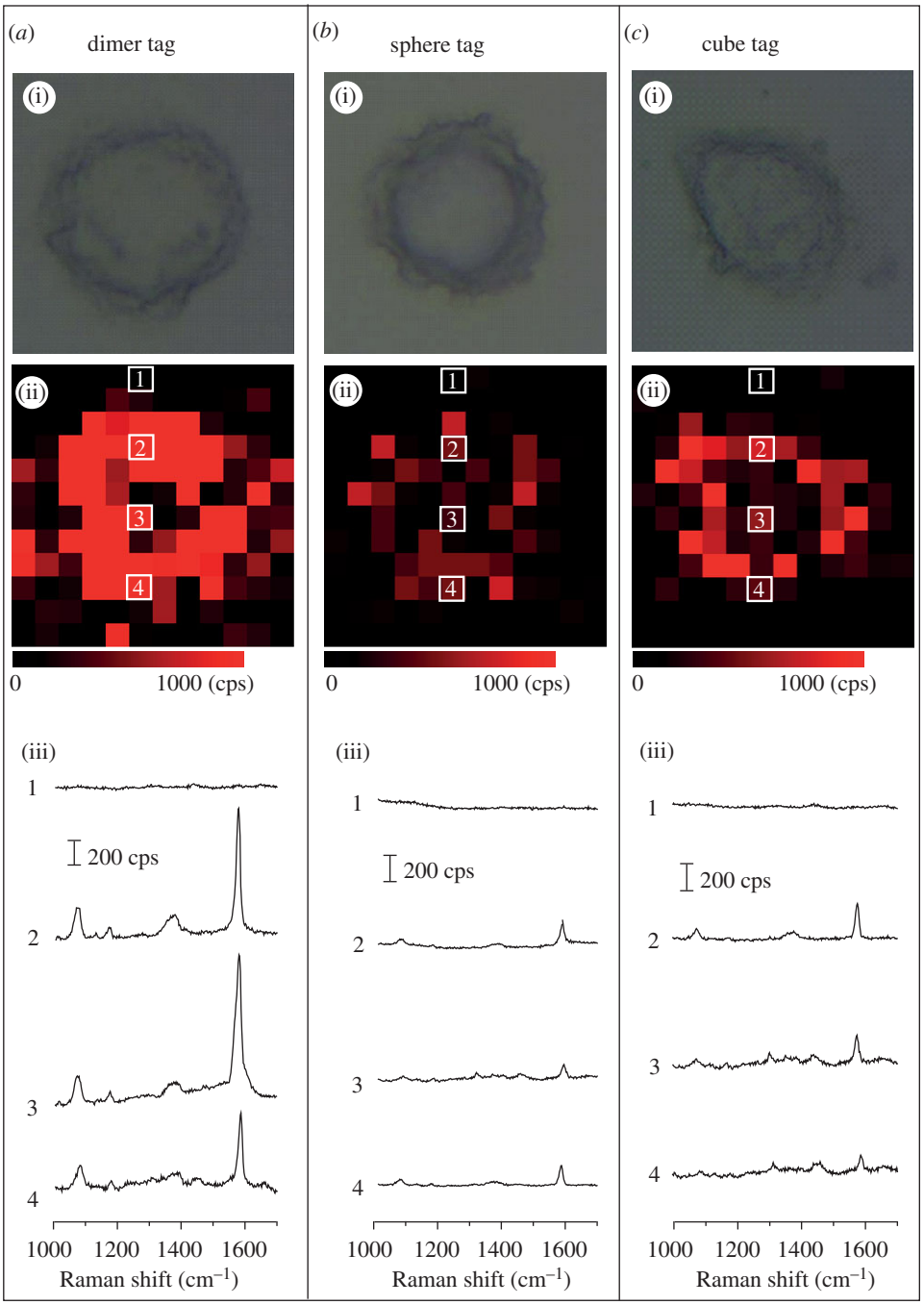

Figure 6. SERS mapping of SK-BR-3 cells by detecting HER2 with: (*a*) dimer tags, (*b*) sphere tags and (*c*) cube tags. In each column, row (i) shows bright-field images of individual cells, and row (ii) shows the corresponding SERS mapping image based on the intensity of the 4-MBA band at 1588 cm^{-1}. The sizes of each image in (i) and (ii) are 24 × 24 μm. (iii) Typical SERS spectra of the SERS mapping image, corresponding to the spots marked with the same numbers in (ii).

S6). These data imply that the dimer tag may be applied to *in vivo* SERS imaging where near-infrared laser excitation is preferred to reduce the background signals from tissues [11].

3.3. Dimer tags for imaging cancer cells

We finally examined the feasibility of using the dimer tags for imaging cancer cells. We chose SK-BR-3 human breast adenocarcinoma cells that overexpress HER2 as a model to demonstrate the SERS imaging capability [47,48], whereas U-87 MG human glioblastoma cells that do not express HER2 were used as a negative control. Prior to SERS imaging, we performed an immunofluorescence assay to determine the HER2 levels on both types of cells, in which HER2 could be resolved through the fluorescence signals coming from fluorescein isothiocyanate (FITC)-labelled secondary antibodies (see electronic supplementary material for experimental details). The images in electronic supplementary material, figure S7 show that the fluorescence of FITC could be detected only for SK-BR-3 cells, confirming the overexpression of HER2 on the surfaces of SK-BR-3 cells and no expression of HER2 for the negative U-87 cells.

Figure 6 shows SERS imaging data of SK-BR-3 cells, using the dimer, sphere and cube tags. In figure 6, row (i) shows bright-field optical microscopy images of individual SK-BR-3 cells; row (ii) shows the corresponding mapping images based on the intensity of the SERS band of 4-MBA at 1588 cm^{-1}; and row (iii) shows typical SERS spectra of different spots on the SERS mapping images, as indicated by the same numbers shown in row (ii). Clearly, the Raman signals of 4-MBA could be detected from SK-BR-3 cells after they had

been incubated with all the three different types of SERS tags. By contrast, the SERS signals of 4-MBA could not be detected from U-87 cells owing to the absence of HER2 receptors on their surface (see the electronic supplementary material, figure S8), indicating the good specificity of the SERS tags. It was found that the dimer tags gave the strongest SERS signal in comparison with the sphere and cube tags in imaging SK-BR-3 cells. To rule out the difference of binding between different tags and cells, we used ICP-MS to determine the number of each type of tag bound to each SK-BR-3 cell right after SERS imaging. Based on the ICP-MS data and the density of cells in each culture well, the average number of tags was roughly estimated to be 1810, 2440 and 2090 per cell for the dimer, sphere and cube tag, respectively. These data suggest that the strongest SERS signal from the dimer-tag-incubated SK-BR-3 cells was mainly caused by the strong SERS enhancement of the dimer tags rather than by a larger number of tag particles bound to each cell. This result demonstrates that the dimer-based tags could be used as a promising SERS imaging agent for cancer diagnosis with good specificity and high sensitivity.

4. Conclusion

In summary, we have demonstrated a new SERS tag based on dimers of Ag nanospheres, which is fabricated by coating dimer of Ag nanospheres with a layer of 4-MBA, a silica shell and antibodies. The dimer tag showed the highest SERS enhancement compared with the tags fabricated from Ag nanospheres and nanocubes with similar sizes. The capability of quantification and good stability was also validated for the dimer tags. The prepared dimer tag was successfully applied to imaging HER2 overexpressing cancer cells with good specificity and high sensitivity. It is expected that the dimer tag mentioned in this study will find its application in SERS imaging for early cancer diagnosis.

This work was supported in part by a Director's Pioneer Award from the NIH (DP1 OD000798), a grant from the NCI (R01 CA13852701). Part of the work was performed at the Nano Research Facility (NRF), a member of the National Nanotechnology Infrastructure Network (NNIN), which is supported by the NSF under award no. ECS-0335765.

References

1. Jeanmaire DL, Van Duyne RP. 1977 Surface Raman spectroelectrochemistry: Part I. Heterocyclic, aromatic, and aliphatic amines. *J. Electroanal. Chem.* **84**, 1–20. (doi:10.1016/S0022-0728(77)80224-6)
2. Kelly KL, Coronado E, Zhao LL, Schatz GC. 2003 The optical properties of metal nanoparticles: the influence of size, shape, and dielectric. *J. Phys. Chem. B* **107**, 668–677. (doi:10.1021/jp026731y)
3. Chang RK, Furtak TE. 1982 *Surface enhanced Raman scattering*. New York, NY: Plenum Press.
4. Campion A, Kambhampati P. 1998 Surface enhanced Raman scattering. *Chem. Soc. Rev.* **27**, 241–250. (doi:10.1039/A827241Z)
5. Isola NR, Stokes DL, Vo-Dinh L. 1998 Surface-enhanced Raman gene probe for HIV detection. *Anal. Chem.* **70**, 1352–1356. (doi:10.1021/ac970901z)
6. Lyandres O, Shah NC, Yonzon CR, Walsh Jr JT, Glucksberg MR, Van Duyne RP. 2005 Real-time glucose sensing by surface-enhanced Raman spectroscopy in bovine plasma facilitated by a mixed decanethiol/mercaptohexanol partition layer. *Anal. Chem.* **77**, 6134–6139. (doi:10.1021/ac051357u)
7. Qian XM *et al*. 2008 *In vivo* tumor targeting and spectroscopic detection with surface-enhanced Raman nanoparticle tags. *Nat. Biotechnol.* **26**, 83–90. (doi:10.1038/nbt1377)
8. Cao YC, Jin R, Mirkin CA. 2002 Nanoparticles with Raman spectroscopic fingerprints for DNA and RNA detection. *Science* **297**, 1536–1540. (doi:10.1126/science.297.5586.1536)
9. Ni J, Lipert RJ, Dawson GB, Porter MD. 1999 Immunoassay readout method using extrinsic Raman labels adsorbed on immunogold colloids. *Anal. Chem.* **71**, 4903–4908. (doi:10.1021/ac990616a)
10. Doering WE, Piotti ME, Natan MJ, Freeman RG. 2007 SERS as a foundation for nanoscale, optically detected biological labels. *Adv. Mater.* **19**, 3100–3108. (doi:10.1002/adma.200701984)
11. Qian XM, Nie SM. 2008 Single-molecule and single-nanoparticle SERS: from fundamental mechanisms to biomedical applications. *Chem. Soc. Rev.* **37**, 912–920. (doi:10.1039/B708839F)
12. Doering WE, Nie SM. 2003 Spectroscopic tags using dye-embedded nanoparticles and surface-enhanced Raman scattering. *Anal. Chem.* **75**, 6171–6176. (doi:10.1021/ac034672u)
13. Keren C, Zavaleta C, Cheng Z, de la Zerda A, Gheysens O, Gambhir SS. 2008 Noninvasive molecular imaging of small living subjects using Raman spectroscopy. *Proc. Natl Acad. Sci. USA* **105**, 5844–5849. (doi:10.1073/pnas.0710575105)
14. Sha MY, Xu H, Natan MJ, Cromer R. 2008 Surface-enhanced Raman scattering tags for rapid and homogeneous detection of circulating tumor cells in the presence of human whole blood. *J. Am. Chem. Soc.* **130**, 17 214–17 215. (doi:10.1021/ja804494m)
15. Lee S, Kim S, Choo J, Shin SY, Lee YH, Choi HY, Ha S, Kang K, Oh CH. 2007 Biological imaging of HEK293 cells expressing PLCγ1 using surface-enhanced Raman microscopy. *Anal. Chem.* **79**, 916–922. (doi:10.1021/ac061246a)
16. Mulvaney SP, Musick MD, Keating CD, Natan MJ. 2003 Glass-coated, analyte-tagged nanoparticles: a new tagging system based on detection with surface-enhanced Raman scattering. *Langmuir* **19**, 4784–4790. (doi:10.1021/la026706j)
17. Maiti KK, Dinish US, Fu CY, Lee J-J, Soh K-S, Yun S-W, Bhuvaneswari R, Olivo M, Chang Y-T. 2010 Development of biocompatible SERS nanotag with increased stability by chemisorption of reporter molecule for *in vivo* cancer detection. *Biosens. Bioelectron.* **26**, 398–403. (doi:10.1016/j.bios.2010.07.123)
18. Ren B, Liu GK, Lian XB, Yang ZL, Tian ZQ. 2007 Raman spectroscopy on transition metals. *Anal. Bioanal. Chem.* **388**, 29–45. (doi:10.1007/s00216-007-1141-2)
19. Talley CE, Jackson JB, Oubre C, Grady NK, Hollars CW, Lane SM, Huser TR, Nordlander P, Halas NJ. 2005 Surface-enhanced Raman scattering from individual Au nanoparticles and nanoparticle dimer substrates. *Nano Lett.* **5**, 1569–1574. (doi:10.1021/nl050928v)
20. Jeong DH, Zhang YX, Moskovits M. 2004 Polarized surface enhanced Raman scattering from aligned silver nanowire rafts. *J. Phys. Chem. B* **108**, 12 724–12 728. (doi:10.1021/jp037973g)
21. Dieringer JA, Lettan RB, Scheidt KA, Van Duyne RP. 2007 A frequency domain existence proof of single-molecule surface-enhanced Raman spectroscopy. *J. Am. Chem. Soc.* **129**, 16 249–16 256. (doi:10.1021/ja077243c)
22. Hao E, Schatz GC. 2004 Electromagnetic fields around silver nanoparticles and dimers. *J. Chem. Phys.* **120**, 357–366. (doi:10.1063/1.1629280)
23. Banholzer MJ, Millstone JE, Qin L, Mirkin CA. 2008 Rationally designed nanostructures for surface-enhanced Raman spectroscopy. *Chem. Soc. Rev.* **37**, 885–897. (doi:10.1039/B710915F)
24. Sun L *et al*. 2007 Composite organic—inorganic nanoparticles as Raman labels for tissue analysis. *Nano Lett.* **7**, 351–356. (doi:10.1021/nl062453t)
25. Huang PJ, Chau LK, Yang TS, Tay LL, Lin TT. 2009 Nanoaggregate-embedded beads as novel Raman labels for biodetection. *Adv. Funct. Mater.* **19**, 242–248. (doi:10.1002/adfm.200800961)
26. Chen J, Jiang J, Gao X, Gong J, Shen G, Yu R. 2007 Gold-aggregated, dye-embedded, polymer-protected nanoparticles (GDPNs): a new type of tags for detection with SERS. *Colloids Surf. A* **294**, 80–85. (doi:10.1016/j.colsurfa.2006.07.049)

27. Lim DK, Jeon KS, Kim HM, Nam JM, Suh YD. 2010 Nanogap-engineerable Raman-active nanodumbbells for single-molecule detection. *Nat. Mater.* **9**, 60–67. (doi:10.1038/nmat2596)
28. Pallaoro A, Braun GB, Reich NO, Moskovits M. 2010 Mapping local pH in live cells using encapsulated fluorescent SERS nanotags. *Small* **6**, 618–622. (doi:10.1002/smll.200901893)
29. Fabris L, Dante M, Nguyen TQ, Tok BBH, Bazan GC. 2008 SERS aptatags: new responsive metallic nanostructures for heterogeneous protein detection by surface enhanced Raman spectroscopy. *Adv. Funct. Mater.* **18**, 2518–2525. (doi:10.1002/adfm.200800301)
30. Li W, Camargo PHC, Au L, Zhang Q, Rycenga M, Xia Y. 2010 Etching and dimerization: a simple and versatile route to dimers of silver nanospheres with a range of sizes. *Angew. Chem. Int. Ed.* **49**, 164–168. (doi:10.1002/anie.200905245)
31. Li W, Camargo PHC, Lu X, Xia Y. 2009 Dimers of silver nanospheres: Facile synthesis and their use as hot spots for surface-enhanced Raman scattering. *Nano Lett.* **9**, 485–490. (doi:10.1021/nl803621x)
32. Zhang Q, Li W, Wen LP, Chen J, Xia Y. 2010 Facile synthesis of Ag nanocubes of 30 to 70 nm in edge length with CF_3COOAg as a precursor. *Chem. Eur. J.* **16**, 10 234–10 239. (doi:10.1002/chem.201000341)
33. Cobley C, Rycenga M, Zhou F, Li Z, Xia Y. 2009 Controlled etching as a route to high quality silver nanospheres for optical studies. *J. Phys. Chem. C* **113**, 16 975–16 982. (doi:10.1021/jp906457f)
34. Xia X, Xu Y, Zhao X, Li Q. 2009 Lateral flow immunoassay using europium chelate-loaded silica nanoparticles as labels. *Clin. Chem.* **55**, 179–182. (doi:10.1373/clinchem.2008.114561)
35. Cho SH, Han HS, Jang DJ, Kim K, Kim MS. 1995 Raman spectroscopic study of 1,4-benzenedithiol adsorbed on silver. *J. Phys. Chem.* **99**, 10 594–10 599. (doi:10.1021/j100026a024)
36. Sisco PN, Murphy CJ. 2009 Surface-coverage dependence of surface-enhanced Raman scattering from gold nanocubes on self-assemble monolayers of analyte. *J. Phys. Chem. A* **113**, 3973–3978. (doi:10.1021/jp810329j)
37. Michota A, Bukowska J. 2003 Surface-enhanced Raman scattering (SERS) of 4-mercaptobenzoic acid on silver and gold substrates. *J. Raman Spectrosc.* **34**, 21–25. (doi:10.1002/jrs.928)
38. Xu Y, Li Q. 2007 Multiple fluorescent labeling of silica nanoparticles with lanthanide chelates for highly sensitive time-resolved immunofluorometric assays. *Clin. Chem.* **53**, 1503–1510. (doi:10.1373/clinchem.2006.078485)
39. Graf C, Vossen DLJ, Imhof A, Blaadern AV. 2003 A general method to coat colloidal particles with silica. *Langmuir* **19**, 6693–6700. (doi:10.1021/la0347859)
40. Liu S, Han M-Y. 2010 Silica-coated metal nanoparticles. *Chem. Asian J.* **5**, 36–45. (doi:10.1002/asia.200900228)
41. Rycenga M, Camargo PHC, Li W, Moran C, Xia Y. 2010 Understanding the SERS effects of single silver nanoparticles and their dimers, one at a time. *J. Phys. Chem. Lett.* **1**, 696–703. (doi:10.1021/jz900286a)
42. McLellan JM, Li Z-Y, Siekkinen AR, Xia Y. 2007 The SERS activity of a supported Ag nanocube strongly depends on its orientation relative to laser polarization. *Nano Lett.* **7**, 1013–1017. (doi:10.1021/nl070157q)
43. McFarland AD, Young MA, Dieringer JA, Van Duyne RP. 2005 Wavelength-scanned surface-enhanced Raman excitation spectroscopy. *J. Phys. Chem. B* **109**, 11 279–11 285. (doi:10.1021/jp050508u)
44. Xia X, Zeng J, McDearmon B, Zheng Y, Li Q, Xia Y. 2011 Silver nanocrystals with concave surfaces and their optical and surface-enhanced Raman scattering properties. *Angew. Chem. Int. Ed.* **50**, 12 542–12 546. (doi:10.1002/anie.201105200)
45. Mulvihill MJ, Ling XY, Henzie J, Yang P. 2010 Anisotropic etching of silver nanoparticles for plasmonic structures capable of single-particle SERS. *J. Am. Chem. Soc.* **132**, 268–274. (doi:10.1021/ja906954f)
46. Rycenga M, Xia X, Moran CH, Zhou F, Qin D, Li Z-Y, Xia Y. 2011 Generation of hot spots with silver nanocubes for single-molecule detection by surface-enhanced Raman scattering. *Angew. Chem. Int. Ed.* **50**, 5473–5477. (doi:10.1002/anie.201101632)
47. Akiyama T, Sudo C, Ogawara H, Toyoshima K, Yamamoto T. 1986 The product of the human c-erbB-2 gene: a 185-kilodalton glycoprotein with tyrosine kinase activity. *Science* **232**, 1644–1646. (doi:10.1126/science.3012781)
48. Kumar R, Shepard HM, Mendelsohn J. 1991 Regulation of phosphorylation of the c-erbB-2/HER2 gene product by a monoclonal antibody and serum growth factor(s) in human mammary carcinoma cells. *Mol. Cell. Biol.* **11**, 979–986. (doi:10.1128/MCB.11.2.979)